

TIFR/TH/99-42  
KIAS/P/99079  
DESY/99-132

## Signature of Charged to Neutral Higgs Boson Decay at the LHC in SUSY Models

Manuel Drees<sup>1</sup>, Monoranjan Guchait<sup>2</sup> and D.P. Roy<sup>3</sup>

<sup>1</sup>IFT, Univ. Estadual Paulista, 01405-900, São Paulo, Brazil

<sup>2</sup>DESY, Notkestrasse 85, D-22607 Hamburg, Germany

<sup>3</sup>TIFR, Homi Bhabha Road, Mumbai - 400 005, India

### Abstract

We study the signature of  $H^\pm$  decay into  $h^0 W$  at the LHC in SUSY models. It has only marginal viability in the MSSM. But in the singlet extensions like the NMSSM one can have a spectacular signature for  $H^\pm$  decay into  $(h^0, A^0)W$  over a significant domain of parameter space.

The minimal supersymmetric Standard Model (MSSM) contains two complex Higgs doublets,  $\phi_1$  and  $\phi_2$ , corresponding to eight scalar states. Three of these are absorbed as Goldstone bosons leaving five physical states – the two neutral scalars ( $h^0, H^0$ ), a pseudo-scalar ( $A^0$ ) and a pair of charged Higgs bosons ( $H^\pm$ ). All the tree-level masses and couplings of these particles are given in terms of two parameters,  $m_{H^\pm}$  and  $\tan\beta$ , the latter representing the ratio of the two vacuum expectation values [1]. While any one of the above neutral Higgs bosons may be hard to distinguish from that of the Standard Model, the  $H^\pm$  carries a distinctive signature of the SUSY Higgs sector. Moreover the couplings of the  $H^\pm$  are uniquely related to  $\tan\beta$ , since the physical charged Higgs boson corresponds to the combination

$$H^\pm = -\phi_1^\pm \sin\beta + \phi_2^\pm \cos\beta. \quad (1)$$

Therefore the detection of  $H^\pm$  and measurement of its mass and couplings are expected to play a very important role in probing the SUSY Higgs sector.

So far the investigations of the  $H^\pm$  signature have been based on its couplings to fermionic channels, which constitute the dominant decay channels of  $H^\pm$  [2,3]. In this note we investigate the  $H^\pm$  signature at LHC in the bosonic decay channel [4]

$$H^\pm \rightarrow Wh^0. \quad (2)$$

Although a subdominant channel for  $H^\pm$  decay, it is important for several reasons.

- i) It is the second most important channel in the low  $\tan\beta$  region for  $m_H > m_t$ , where the dominant decay channel [2]

$$H^+ \rightarrow t\bar{b} \quad (3)$$

suffers from a large irreducible background from the QCD processes

$$gg \rightarrow t\bar{t}g, \quad gq \rightarrow t\bar{t}q, \quad gb \rightarrow t\bar{t}b. \quad (4)$$

- ii) The fermionic couplings of  $H^\pm$  hold for any two Higgs doublet model of type II [1], i.e. where  $H^\pm$  represents the combination (1). In contrast the prediction of  $H^\pm$  coupling to the  $Wh^0$  channel in terms of  $\tan\beta$  and  $m_{H^\pm}$  holds only in the MSSM and hence serves as a unique test of this model.

- iii) Moreover, unlike its fermionic couplings the  $H^\pm$  coupling to  $Wh^0$  is sensitive to the singlet extensions of the MSSM, like the next-to-minimal supersymmetric Standard Model [5,6] (NMSSM). Therefore this signature would be useful in probing such models. In fact we shall see below that the signature is expected to have only marginal viability in the MSSM, while in NMSSM it can be quite spectacular over a significant part of the parameter space.

For calculating the branching fraction for  $H^\pm \rightarrow Wh^0$  decay, we shall use the radiatively corrected MSSM relation between  $H^\pm$  and  $h^0$  masses including the effect of stop mixing [7]. It is only for very large values of the stop mass and mixing parameters that the  $h^0$  masses can escape the LEP-2 limit in the low  $\tan\beta$  region of our interest [8]. We shall therefore assume a large stop mass of  $\sim 1$  TeV along with maximal mixing. The relevant formulae for this decay branching fraction can be found in the paper of Djouadi, Kalinowski and Zerwas [4]. The resulting branching fractions are shown as functions of  $\tan\beta$  in Fig. 1 for several  $H^\pm$  masses. In each case the region to the left of the cross will be excluded by the nonobservation of  $h^0$  at LEP-2 at the end of the 200 GeV run. In fact the present exclusion limits of LEP-2 are close to these values.

Fig. 1 shows that the  $H^\pm \rightarrow Wh^0$  decay branching fraction is at best 8–9% for  $m_{H^\pm} = 200$  GeV, i.e. just above the  $t\bar{b}$  threshold, and goes down rapidly with increasing  $m_{H^\pm}$ . Note that even below the  $t\bar{b}$  threshold (dashed line) this branching fraction remains  $\leq 4$ –5% over the LEP-2 allowed region. The latter corresponds to  $m_h > 100$  GeV, which means that  $m_{H^\pm}$  is also below the  $Wh^0$  threshold. The dominant decay channel in this case is  $H^\pm \rightarrow \tau\nu$  [3,4]. We shall see below however that the LEP-2 constraints on the  $h^0, A^0$  masses are far less severe in the NMSSM. Consequently a  $H^\pm$  below the  $t\bar{b}$  threshold can decay into on-shell  $Wh^0(A^0)$ , which would then be the dominant decay channel.

For  $m_H > m_t$  the dominant process of  $H^\pm$  production at LHC is its associated production with top. We shall be using the LO production mechanism

$$gb \rightarrow tH^- + \text{h.c.} \quad (5)$$

for computing the signal cross-section. It is controlled by the Yukawa cou-

pling at the  $tbH$  vertex,

$$\frac{g}{\sqrt{2}m_W} H^+ [\cot \beta m_t \bar{t} b_L + \tan \beta m_b \bar{t} b_R] + \text{h.c.} \quad (6)$$

Consequently it goes down like  $1/\tan^2 \beta$  over the low  $\tan \beta$  region of our interest. The electro-weak loop correction to this cross-section has been estimated to give upto 20% reduction in this region [9]. The corresponding QCD correction is expected to be larger, but not yet available. It may be noted here that the SUSY QCD correction to the  $H^\pm$  signal cross-section could be large and of either sign depending on the choice of SUSY parameters [10]. For simplicity we shall neglect this by assuming a large SUSY mass scale  $\sim 1$  TeV, which is consistent with our assumption of stop mass. Finally, the cross-section from  $gg \rightarrow tbH^-$  is about half that of the LO process (5). Adding the two contributions and subtracting out the overlapping piece seems to give a net signal cross-section midway between the two values, i.e. about 2/3rd the LO Cross-section [11]. We shall be neglecting this correction to the LO cross-section as well.

Our analysis is based on a parton level Monte Carlo program. The LO cross-section for (5) is convoluted with the LO parton densities of CTEQ-4L [12] to generate the  $tH^-$  signal. This is followed by the decay sequence

$$tH^- \rightarrow bWh^0W \rightarrow b\bar{b}\ell\nu q\bar{q}, \quad (7)$$

i.e.  $h^0 \rightarrow b\bar{b}$  while one  $W$  decays leptonically and the other hadronically. Thus the final state consists of 3  $b$ -tagged and 2 untagged jets along with a hard lepton and missing  $p_T$  ( $\not{p}_T$ ). We consider the background coming from the dominant decay channel (3) as well as the QCD processes (4). We have tried to simulate detector resolution by a gaussian smearing of all the jet momenta, with

$$(\sigma(p_T)/p_T)^2 = (0.6/\sqrt{p_T})^2 + (0.04)^2. \quad (8)$$

The  $\not{p}_T$  is obtained by vector addition of all the  $p_T$ 's after resolution smearing.

As a basic set of selection cuts we require

$$p_T > 30 \text{ GeV} \quad \text{and} \quad |\eta| < 2.5 \quad (9)$$

for all the jets and the lepton, where  $\eta$  denotes pseudorapidity and the  $p_T$ -cut is applied to  $\not{p}_T$  as well. We also require a minimum separation of

$$\Delta R = [(\Delta\phi)^2 + (\Delta\eta)^2]^{1/2} > 0.4 \quad (10)$$

between the lepton and the jets as well as each pair of jets. We require that exactly three  $b$ -quarks in the final state (7) are tagged, assuming a  $b$ -tagging efficiency of 50%. We take a mis-tagging probability of 1% for light quark and gluon jets when estimating the signal and background cross-sections.

Then the signal and background events are subjected to the following mass reconstructions.

- (a) The invariant mass of the two untagged jets is required to be consistent with  $m_W \pm 15$  GeV, and the resulting  $W$  is reconstructed from their momenta.
- (b) For the leptonically decaying  $W$  the  $p_L(\nu)$  and the resulting  $p_L(W)$  are determined within a quadratic ambiguity using the constraint  $m_W = m(\ell\nu)$ . In the case of complex solutions the imaginary part is discarded and the solutions coalesce.
- (c) One of the reconstructed  $W$ 's is required to combine with one of the  $b$ 's to give an invariant mass  $= m_t \pm 25$  GeV. In case of several combinations satisfying this constraint, the one closest to  $m_t$  ( $= 175$  GeV) is selected. The corresponding  $b$  and  $W$  are identified with the reconstructed top.
- (d) The remaining  $b$ -pair is required to have an invariant mass  $= m_h \pm 10$  GeV. This constraint helps to suppress the backgrounds from (3) and (4).
- (e) Moreover we require that the invariant mass of the remaining  $W$  with neither of this  $b$ -pair should lie within  $m_t \pm 20$  GeV. This veto on the second top mass helps to suppress the backgrounds further.
- (f) Finally the  $H^\pm$  mass is reconstructed by combining this  $W$  with the  $b$ -pair. In case this  $W$  has a quadratic ambiguity both the invariant masses are retained. Of course only one of these will correspond to the actual  $H^\pm$  mass.

Fig. 2 shows the signal and background cross-sections against this  $Wbb$  invariant mass for  $m_{H^\pm} = 220$  GeV and  $\tan\beta = 2$  – i.e. for a  $H^\pm$  mass just above the  $t\bar{b}$  threshold and  $\tan\beta$  just above the corresponding exclusion range of LEP-2. The mass constraints have helped to suppress both the backgrounds by at least an order of magnitude each without any serious loss

to the signal cross-section. Consequently the signal/background ratio is  $\sim 1$  in the region of the  $H^\pm$  mass peak in the signal. Unfortunately the signal size is rather marginal. It corresponds to a cross-section of  $.04 \text{ fb}$  – i.e. about a dozen events for an accumulated luminosity of  $300 \text{ fb}^{-1}$ , corresponding to 3 years of LHC run at high luminosity. It should be mentioned here that this choice of  $H^\pm$  mass and  $\tan\beta$  represents by far the most favourable combination for the  $H^\pm \rightarrow Wh^0$  signal (see Fig. 1). Increasing the  $H^\pm$  mass from 220 to 300 GeV reduces the decay branching fraction by a factor of 3 and the overall signal size by a factor of  $\sim 5$ . While there is a small increase in the branching fraction with  $\tan\beta$ , it would be more than offset by the corresponding drop in the  $H^\pm$  production cross-section (5).

We have also investigated the signal for  $m_{H^\pm} = 160 \text{ GeV}$  at  $\tan\beta = 3$ , i.e. at the edge of the LEP-2 exclusion range. Here the main contribution to the signal comes from

$$\bar{t}t \rightarrow \bar{t}bH^+, \quad (11)$$

followed by the decay chain (7). The additional  $b$  in (11) is found to be too soft to survive the  $p_T > 30 \text{ GeV}$  cut. Thus the final state is practically the same as in (7), except that one of the two  $W$ 's is off-shell. Nontheless it is possible to do a complete reconstruction by requiring leptonic decay for the on-shell  $W$ . The reconstructed masses are then subjected to the  $m_t$  and  $m_h$  constraints as before. The resulting signal is again found to be of similar size as in Fig. 2, i.e. only  $\sim .05 \text{ fb}$ . The main reason for this is that the  $t \rightarrow bH^+$  branching fraction in this case is only 0.4%. Thus the  $H^\pm \rightarrow Wh^0$  decay signal is expected to be of only marginal size, and that too over a limited range of the MSSM parameters,  $m_{H^\pm}$  and  $\tan\beta$ .

One can have a more favourable signal in singlet extensions of the MSSM, where the LEP constraints on the Higgs boson masses are far less severe. Thus it is possible to have a  $H^\pm$  lighter than top for any value of  $\tan\beta$  down to 1.5; and it is possible for this  $H^\pm$  to decay into a on-shell  $Wh^0$  and/or  $WA^0$  pair [13]. In this case  $H^\pm \rightarrow Wh^0(A^0)$  is expected to be the dominant decay channel, resulting in a spectacular signal at LHC.

Two types of singlet extensions of the MSSM have been extensively discussed in the literature. The first is based on a  $U(1)$  extension of the SM gauge group, which is inspired by  $E(6)$  GUT [14,15]. The second only extends the Higgs sector of the MSSM by adding a complex singlet superfield  $N$ . This is the above mentioned NMSSM, which is widely recognised as of-

fering a natural solution to the so-called  $\mu$ -problem of the MSSM [5,6]. We shall be concentrating on this second model.

In the NMSSM the Higgs self-interaction is described by two cubic terms in the superpotential, i.e.

$$\lambda NH_1H_2 - \frac{k}{3}N^3 \quad (12)$$

using the notation of [6]. Together with the corresponding soft breaking terms,  $A_\lambda$  and  $A_k$ , and the singlet vev  $\langle N \rangle$ , there are 5 free parameters in addition to  $\tan\beta$ . Thus the Higgs sector is less constrained than that of the MSSM, where we had only one other free parameter ( $m_{H^\pm}$ ) along with  $\tan\beta$ . Consequently the MSSM mass relations among the physical Higgs particles and the resulting indirect mass limits from LEP are no longer valid. Moreover we have to add a singlet scalar and a pseudoscalar, which will mix with the corresponding doublet states diluting the direct mass bound on the latter from LEP.

We have numerically scanned the above 5 parameters to obtain solutions which give maximal branching fractions for

$$H^\pm \rightarrow W(h_1^0, A_1^0) \quad (13)$$

for fixed input values of  $\tan\beta$  and fixed output ranges of  $m_{H^\pm}$  [13]. Here the subscript 1 denotes the lightest scalar (pseudoscalar) state. The radiative correction has been included assuming a large stop mass of  $\sim 1$  TeV and maximal stop mixing as in the earlier case. We have included the final exclusion limits of LEP-2 along with those from LEP-1. Moreover we have also required that the desired minimum of the Higgs potential, where all the three neutral Higgs fields have non-zero vev, is the absolute minimum of the potential. This physical requirement helps considerably in constraining the parameter space.

Table I shows the optimal solutions with  $M_{H^\pm} \sim 160$  GeV for fixed values of  $\tan\beta = 2, 2.5$  and  $3$ . It should be noted that these solutions are obtained with reasonable values of the singlet vev and coupling parameters. The resulting  $h_1$  and  $A_1$  masses are shown along with the corresponding branching fractions. For each  $\tan\beta$ , we show two solutions where  $H^\pm \rightarrow Wh_1$  and  $H^\pm \rightarrow WA_1$  are the dominant decay channels. Note that for dominant  $H^\pm \rightarrow Wh_1$  solutions the  $h_1$  mass is always close to the LEP-1 bound from

the  $Z^*h$  final state. Thanks to the large event rate, the LEP-1 limit on  $m_h$  is far more robust than the corresponding limit from LEP-2. Any  $h^0$  with a non-negligible doublet component cannot lie much below the former limit. In contrast there is no direct limit on  $A^0$  from LEP in the low  $\tan\beta$  region. We have only associated production of  $h^0A^0$ ; and even this is strongly suppressed in the low  $\tan\beta$  region. There is an indirect limit obtained from the LEP limit on  $m_h$  using the MSSM mass relation, which is not valid here. Consequently even a doublet pseudoscalar can be very light in this model. This explains why the optimal  $H^\pm \rightarrow WA_1^0$  solutions favour so low values of  $A_1^0$  mass. Indeed this may be the most promising process for  $A^0$  search in the low  $\tan\beta$  region.

We have estimated the signal cross-section from  $t\bar{t}$  production, followed by the decays (11) and (7). As mentioned before, the accompanying  $b$  in (11) is too soft to survive the  $p_T > 30$  GeV cut, so that the final state is practically the same as (7), with both  $W$ 's on-shell. We apply the same selection cuts and invariant mass constraints as before. The resulting signal cross-sections are listed in the last column. We have not listed the signal size for the light  $A_1$  solutions, because the small value of  $m_{A_1}$  makes it very sensitive to the choice of  $\Delta R$  (10). Of course such small values of  $m_{A_1}$  are picked up because of the requirement of maximal  $B_{A_1}$ , which is the branching fraction of  $H^\pm$  to  $WA_1$ , in our optimization program. One can easily raise  $m_{A_1}$  to  $\sim 50$  GeV without much reduction to the resulting  $B_{A_1}$ . The resulting signal would then be of similar size as the listed ones.

The signal size is  $\sim 2$  fb, corresponding to about 200 events for an annual luminosity  $100 \text{ fb}^{-1}$  at LHC. Evidently these would be very spectacular events, consisting of 3  $b$ 's and 2  $W$ 's. While one of the  $W$ 's should combine with one of the  $b$ 's to form the  $m_t$  peak, the remaining  $b$ -pair should show the  $m_h(m_A)$  peak and also combine with the remaining  $W$  to form the  $m_{H^\pm}$  peak. We have also checked that one can get similar solutions for still smaller values of  $m_{H^\pm}$  ( $= 140 - 150$  GeV) as well as  $\tan\beta$  ( $= 1.5$ ), which would correspond to still larger signals.

**Acknowledgements:** This work was started at the Les Houches Workshop on Physics at TeV colliders, organised by LAPP, Annecy. We thank the organisers, Patrick Aurenche and Fawzi Boudjema, for a very stimulating workshop. The authors are thankful to Peter Zerwas and Michael Spira for useful suggestions and Rajeev Bhalerao for computational advice. The work

of MG was supported by the Alexander von Humboldt Fellowship while that of DPR was partly supported by the IFCPAR under project No. 1701-1. MD thanks the School of Physics of KIAS, Seoul, for their hospitality while this work was completed.

## References

- [1] J.F. Gunion, H.E. Haber, G.L. Kane and S. Dawson, “The Higgs Hunters’ Guide” (Addison-Wesley, Reading, MA, 1990).
- [2] J.F. Gunion, Phys. Lett. B322 (1994) 125; V. Barger, R.J.N. Phillips and D.P. Roy, Phys. Lett. B324 (1994) 236; D.H. Miller, S. Moretti, D.P. Roy and W.J. Stirling, hep-ph/9906230.
- [3] S. Raychaudhuri and D.P. Roy, Phys. Rev. D52 (1995) 1556; D53 (1996) 4902; M. Guchait and D.P. Roy, Phys. Rev. D55 (1997) 7263; E. Keith, E. Ma and D.P. Roy, Phys. Rev. D56 (1997) R5306; E. Ma, D.P. Roy and J. Wudka, Phys. Rev. Lett. 80 (1998) 1162; D.P. Roy, Phys. Lett. B459 (1999) 607.
- [4] S. Moretti and W.J. Stirling, Phys. Lett. B347 (1995) 291, Erratum *ibid*, B366 (1996) 451; A. Djouadi, J. Kalinowski and P.M. Zerwas, Z. Phys. C70 (1996) 435.
- [5] H.P. Nilles, M. Srednicki and D. Wyler, Phys. Lett. 120B (1983) 346; M. Drees, Int. J. Mod. Phys. A4 (1989) 3635; J. Ellis, J.F. Gunion, H.E. Haber, L. Roszkowski and F. Zwirner, Phys. Rev. D39 (1989) 844; U. Ellwanger and M. Rausch de Traubenberg, Z. Phys. C53 (1992) 521; P.N. Pandita, Z. Phys. C59 (1993) 575; Phys. Lett. B318 (1993) 338; T. Elliot, S.F. King and P.L. White, Phys. Rev. D49 (1994) 2435.
- [6] S.F. King and P.L. White, Phys. Rev. D52 (1995) 4183; D53 (1996) 4049.
- [7] H.E. Haber, R. Hempfling and A.H. Hoang, Z. Phys. C75 (1997) 539. M. Carena, J. Espinosa, M. Quiros and C. Wagner, Phys. Lett. B355 (1995) 209.

- [8] see e.g. ALEPH Collaboration: R. Barate et. al., *Phys. Lett.* B440 (1998) 419.
- [9] L.G. Jin, C.S. Li, R.J. Oakes and S.H. Zhu, [hep-ph/9907482](#).
- [10] J.A. Coarasa, D. Garcia, J. Guasch, R.A. Jimenez and J. Sola, *Eur. Phys. J.* C2 (1998) 373; *Phys. Lett.* B425 (1998) 329.
- [11] F. Borzumati, J. L. Kneur and Nir Polonsky, [hep-ph/9905443](#).
- [12] CTEQ Collaboration: H.L. Lai et. al., *Phys. Rev.* D55 (1997) 1280.
- [13] M. Drees, E. Ma, P.N. Pandita, D.P. Roy and S. Vempati, *Phys. Lett.* B433 (1998) 346.
- [14] For a review, see J.L. Hewett and T.G. Rizzo, *Phys. Rep.* 183 (1989) 193.
- [15] H.E. Haber and M. Sher, *Phys. Rev.* D35 (1987) 2206; M. Drees, *Phys. Rev.* D35 (1987) 2910; V. Barger and K. Whisnant, *Int. J. Mod. Phys.* A3 (1988) 1907; E. Keith and E. Ma, *Phys. Rev.* D54 (1996) 3587; D56 (1997) 7155.

$\tan \beta$	$M_{H^\pm}$ (GeV)	$B_{H^\pm}$ (%)	$\langle N \rangle$ (GeV)	$\lambda, k$	$A_\lambda, A_k$ (GeV)	$m_{h_1}, m_{A_1}$ (GeV)	$B_{h_1}, B_{A_1}$ (%)	$\sigma_{H^\pm}$ (fb)
2	164	0.4	147	.39,-.25	-158,-59	56,36	51,43	2
	160	0.8	273	.40,-.73	12, 8	115,15	0,97	—
2.5	160	0.5	231	.21,-.41	-101,111	51,137	86,0	2.2
			278	.33,-.72	16,8	113,15	0,95	—
3	160	0.4	196	.14,-.33	-184,-8	54,27	69,16	1.6
			341	.22,-.62	23, 6	110,19	0,90	—

Table I - Maximal branching fractions for  $H^\pm \rightarrow W(h_1^0, A_1^0)$  decay in the NMSSM for fixed input values of  $\tan \beta$  and output  $H^\pm$  mass of  $\sim 160$  GeV. The values of the  $h_1^0, A_1^0$  masses and these branching fractions are shown along with the corresponding model parameters. Also shown are the  $t \rightarrow bH^\pm$  branching fraction and the size of the resulting  $H^\pm \rightarrow W(h_1^0, A_1^0)$  decay signal at LHC.

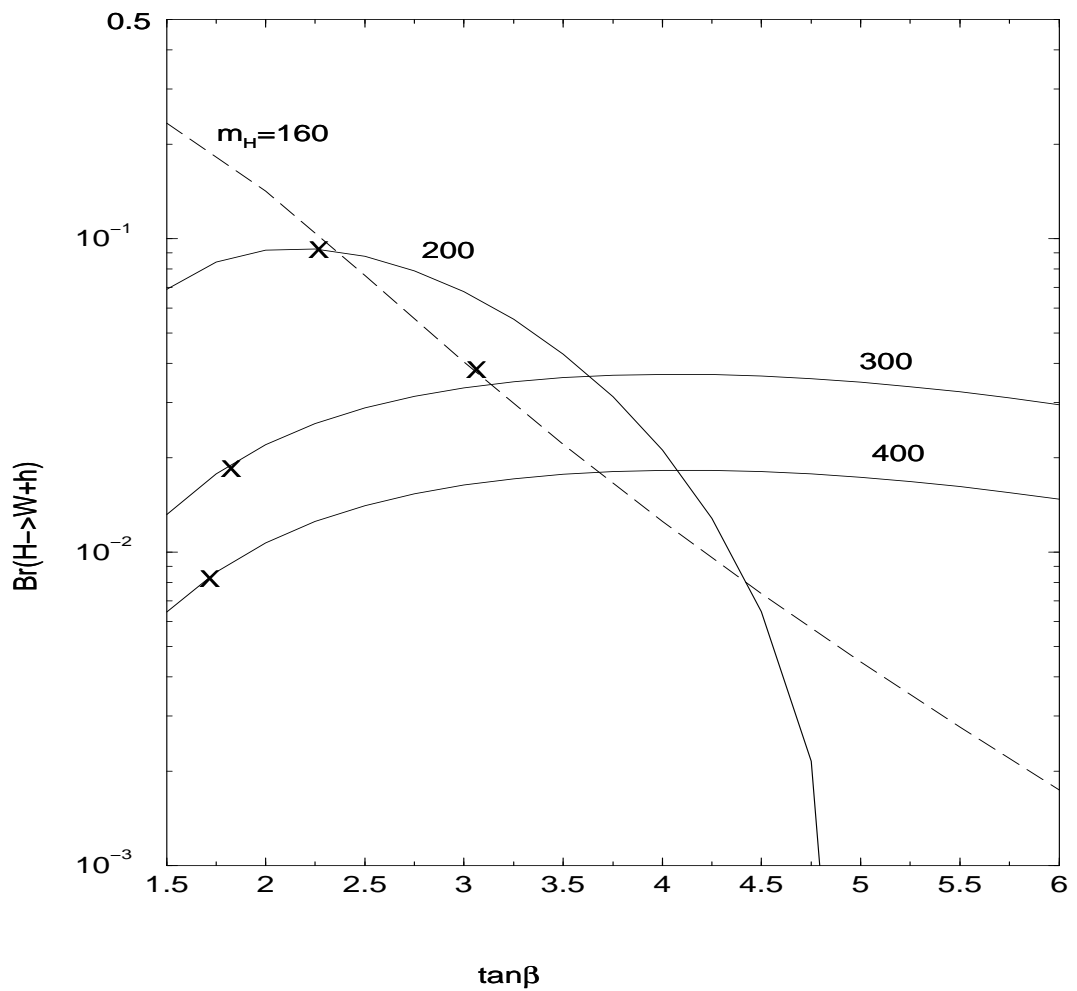


Figure 1: Branching fraction of  $H^\pm \rightarrow Wh^0$  decay is shown against  $\tan\beta$  for different  $H^\pm$  masses. In each case the LEP-2 exclusion limit of  $\tan\beta$  is indicated by the cross.

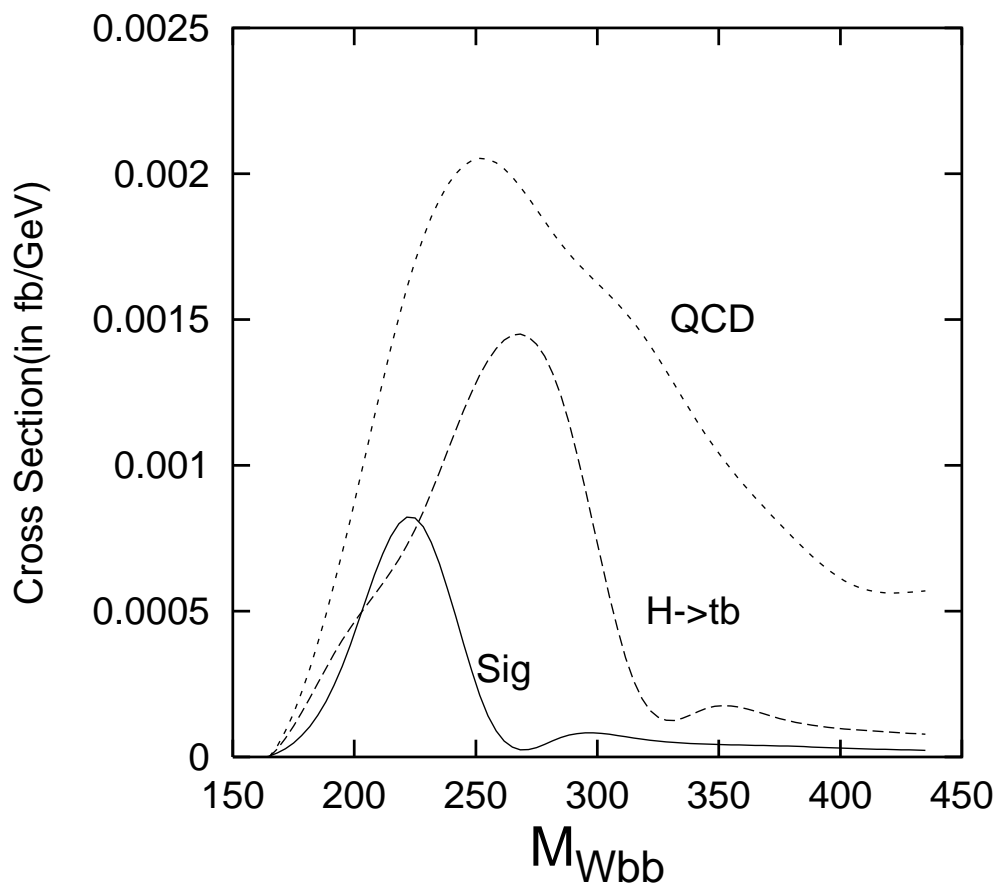


Figure 2: The  $H^\pm \rightarrow Wh^0$  signal cross-section at LHC is shown against the reconstructed  $H^\pm$  mass for  $m_{H^\pm} = 220$  GeV and  $\tan\beta = 2$  along with  $H^\pm \rightarrow t\bar{b}$  and the QCD backgrounds.